Int. J. Adv. Appl. Math. and Mech. 7(3) (2020) 1 – 10 (ISSN: 2347-2529)

Journal homepage: www.ijaamm.com

IJAAMM

International Journal of Advances in Applied Mathematics and Mechanics

Mathematical Modelling & Optimization of Crew Module-Service Module Umbilical Separation Mechanism for Manned Mission

Research Article

Lala Surya Prakash[a, *], Chandan Saxena [b], Dilip V [b], Krishnanandan V [a]

[a] *Human Space Flight Group, Liquid Propulsion Systems Centre, Indian Space Research Organisation, Valiamala-695547, Kerala, India*

[b] *Control Systems & Umbilical Division, Liquid Propulsion Systems Centre, Indian Space Research Organisation, Valiamala-695547, Kerala, India*

Received 24 December 2019; accepted (in revised version) 12 February 2020

Abstract: A simplified dynamic model is formulated for the actuator-boom configuration, proposed for the separation of umbilical system interconnecting Crew Module and Service Module. Optimization studies are carried out using open-source *SciPy* library on *Python* platform. The objective of this study is to estimate the force, to be delivered by actuator, to separate the umbilical system from Crew Module with constraints imposed from mission and launch vehicle. This study does not cover the structural optimization aspects. However, it provides promising inputs and insight to proceed with configuration and design of the system.

MSC: 70E17 • 49K21 • 90C90

Keywords: Mathematical Modeling • Optimization • Umbilical • Crew Module • Service Module

1. Introduction

Indian Space Research Organization (ISRO) has initiated manned mission program to achieve in-house human space flight capability [1]. Towards this, Crew Module (CM) and Service Module (SM) are proposed to carry crew to orbit and return them safely back to a pre-determined location. CM serves as the habitat of crew and SM caters for life support and propulsion requirements during ascent and on-orbit phases of the mission. A umbilical system is proposed to facilitate fluid and electrical interconnection between CM and SM till the time of CM-SM separation. The CM is located above SM and umbilical system interconnects CM-SM from outside the CM-SM structure (Fig. 1).

CM has ablative liner as heat shield for combating heat during re-entry. As CM re-enters atmosphere facing bottom, the umbilical lines cannot be routed through the bottom without affecting the heatshield. The only alternative available is to route the lines outside (Fig. 1). The proposed umbilical system consists of Umbilical Plate sub-assembly, Boom, and Actuator. Umbilical plate sub-assembly, which houses fluid/electrical connectors, consists of two plates in mated condition during operation. One plate is mounted on the fore-end of the actuatable boom and other half is fixed to CM. The fluid/electrical lines are routed from SM to CM though the boom structure. The boom is a rigid arm with planar rotational degree of freedom about the fixed mounting point located at SM fore-end. The actuator provide the necessary force for separation of umbilical system from CM prior to separation of SM during abort and descent phase (around 120 km altitude) of the mission.

* Corresponding author.

E-mail address(es): jacobian18@gmail.com, ls_prakash@lpsc.gov.in (Lala Surya Prakash), chandan_saxena@lpsc.gov.in (Chandan Saxena), v_dilip@lpsc.gov.in (Dilip V), v_krishnanandan@lpsc.gov.in (Krishnanandan V).

Nomenclature

CM	Crew Module
SM	Service Module
CG	Center of gravity
b	length of the umbilical plate in plane of rotation
F_a	Force delivered by actuator
F_g	Gravity force on total boom
I	Moment of Inertia of total boom w.r.t origin
I_c	Moment of Inertia of boom part on CM w.r.t origin
I_m	Moment of Inertia of boom part outside CM w.r.t origin
I_p	Moment of Inertia of umbilical plate sub-assembly w.r.t origin
X	Horizontal distance between mounting points of actuator and boom
X_{max}	Maximum horizontal space available to accomodate umbilical system
X_{sp}	Horizontal distance between mounting points of actuator and actuator-boom joint
X^*	Matrix representing optimal solution
Y	Vertical distance between mounting points of actuator and boom
Y_{gap}	Vertical gap between actuator-boom joint and SM top
Y_{max}	Maximum vertical space available to accomodate umbilical system
Y_{sp}	Vertical distance between mounting points of actuator and actuator-boom joint
f	Function representing objective function
g_i	Inequality constraints
m	Total mass of the boom including fluid/electrical lines
m_c	Mass of the boom part which lies on CM
m_p	Mass of the umbilical plate sub-assembly
m_m	Mass of the boom part which lies outside the boom and acts as moment arm for actuator
$\vec{r}_{cg}$	CG of the total boom
t	Time
t_{sep}	Time required for full separation of umbilical system from CM
x_{cg}	Abscissa of CG of the total boom
$x_{c,cg}$	Abscissa of CG of the boom part which lies on CM
$x_{m,cg}$	Abscissa of CG of the boom part which lies outside of CM
$x_{p,cg}$	Abscissa of CG of the umbilical plate
y_{cg}	Ordinate of CG of the total boom
$y_{c,cg}$	Ordinate of CG of the boom part which lies on CM
$y_{m,cg}$	Ordinate of CG of the boom part which lies outside of CM
$y_{p,cg}$	Ordinate of CG of the umbilical plate
l_a	Length of the actuator in non-actuated condition
l_c	Length of the boom part on CM
l_m	Length of the boom part outside CM
l_p	Distance of CG of umbilical plate from top end of the boom ($l_p = 0.5b$ for present study)
α	Angular acceleration of boom w.r.t origin
β	Angle made by actuator w.r.t x-axis in non-actuated position
θ	Angle made by boom part outside CM w.r.t x-axis
θ_c	Angle made by boom part on CM w.r.t x-axis
θ_{cf}	Final angle made by boom part on CM w.r.t x-axis after separation
θ_f	Final angle made by boom part outside CM w.r.t x-axis after separation
ω	Angular velocity of boom w.r.t origin
τ	Net torque applied on boom w.r.t origin

National Aeronautics and Space Administration (NASA), USA has developed actuator based umbilical separation mechanism for Apollo and Orion programs. Apollo's CSM [2] and Orion spacecraft [3] routed their umbilical lines outside from Service Module to Command Module.

The launch vehicle envelope and mission constraints are major factors deciding the design of the umbilical system. This paper presents the details of mathematical modelling and optimization study carried out for the proposed actuator-boom configuration.

2. Development of Mathematical Model

The actuator-boom configuration is similar to one employed in hydraulic excavators. Ref. [4] and [5] are referred for the development of the mathematical model of actuator-boom. In the present study, the boom is modelled as bent

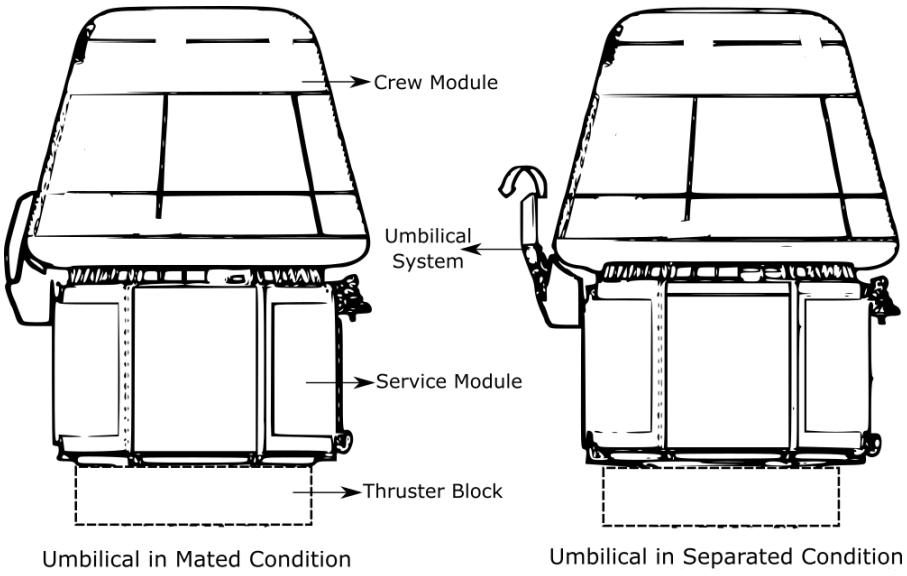

Fig. 1. Overall configuration of CM-SM Umbilical

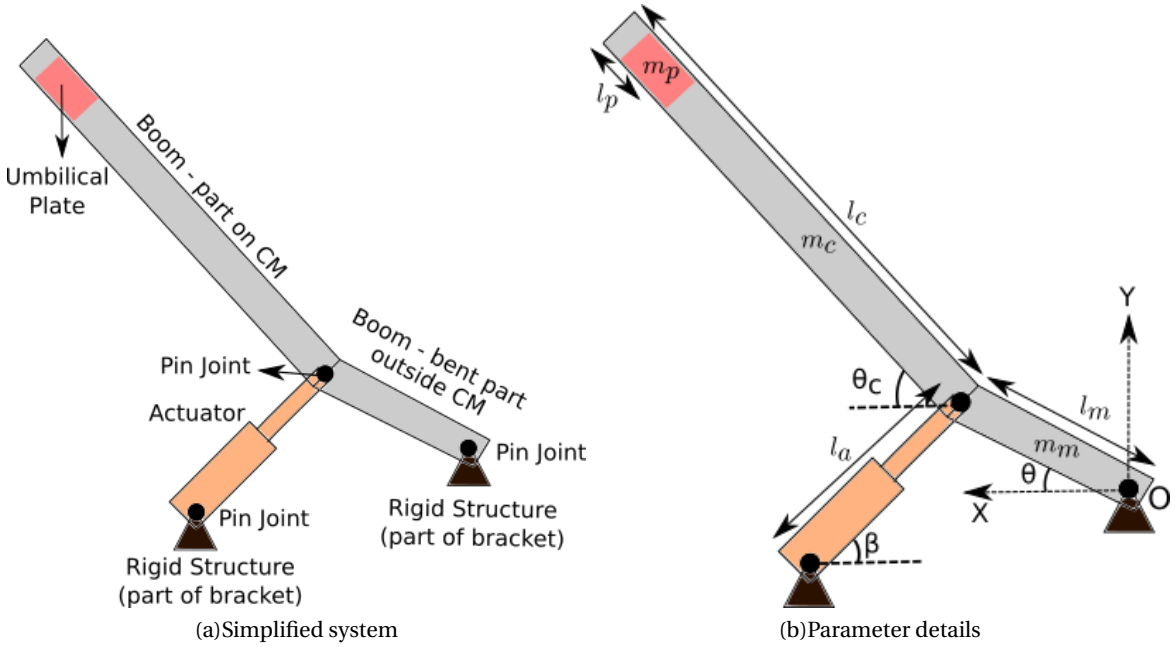

(a)Simplified system (b)Parameter details

Fig. 2. Kinematic details of boom-actuator system

beam structure for generalization.

The boom is assumed as a rigid structure with non-uniform load distribution due to the umbilical plate and fluid/electrical lines. In order to parametrize this non-uniform load, the loads are assumed to be concentrated at three locations on the beam (Fig. 2(a)) umbilical plate sub-assembly (b) part of the boom which lies on CM (c) part of the boom outside the CM which acts as moment arm for actuator. In order to maximize the moment arm, the point of action of the actuator is proposed to coincide with the point of bend. Total mass of the boom-actuator system is expressed as -

$$m = m_p + m_c + m_m \tag{1}$$

2.1. Center of gravity of the boom

The center of gravity (CG) of total boom structure, including boom, electrical/fluid lines and umbilical plate, is specified in vector form w.r.t XY cartesian co-ordinate system with origin (0,0) at point 'O' (Fig. 2(b)).

$$\vec{r}_{cg} = x_{cg}\,\hat{i} + y_{cg}\,\hat{j} \tag{2}$$

where,

$$\begin{aligned} x_{cg} &= \frac{x_{m,cg}m_m + x_{c,cg}m_c + x_{p,cg}m_p}{m_m + m_c + m_p} \\ &= \frac{1}{m}\left[0.5m_m l_m \cos\theta + m_c\left(l_m\cos\theta + 0.5l_c\cos\theta_c\right) + m_p\left(l_m\cos\theta + \left(l_c - l_p\right)\cos\theta_c\right)\right] \end{aligned}$$

$$\begin{aligned} y_{cg} &= \frac{y_{m,cg}m_m + y_{c,cg}m_c + y_{p,cg}m_p}{m_m + m_c + m_p} \\ &= \frac{1}{m}\left[0.5m_m l_m \sin\theta + m_c\left(l_m\sin\theta + 0.5l_c\sin\theta_c\right) + m_p\left(l_m\sin\theta + \left(l_c - l_p\right)\sin\theta_c\right)\right] \end{aligned}$$

2.2. Moment of Inertia of the Boom

Moment of inertia (MI) of the total boom about origin point 'O' is expressed as

$$I = I_m + I_c + I_b \tag{3}$$

where,

$$\begin{aligned} I_m &= \frac{m_m l_m^2}{3} \\ I_c &= m_c\left[l_m^2 + \frac{l_c^2}{3} + l_m l_c\cos\left(\theta_c - \theta\right)\right] \\ I_p &= \frac{m_p b^2}{12} + m_p\left[l_m^2 + \left(l_c - l_p\right)^2 + 2l_m\left(l_c - l_p\right)\cos\left(\theta_c - \theta\right)\right] \end{aligned}$$

2.3. Kinematics

In order to meet the separation requirements, the boom need to rotate to a final position of θ_{cf} in a time t_{sep} imposed by mission. As the expressions for MI and CG are in terms of θ, θ_{cf} is converted to θ_f using geometric relationship (4).

$$\theta_{cf} = \theta_f + (\theta_c - \theta) \implies \theta_{cf} - \theta_c = \theta_f - \theta \tag{4}$$

Assuming constant angular acceleration, the following holds true.

$$\theta_f = \theta + \omega_o t_{sep} + \frac{1}{2}\alpha t_{sep}^2$$

As the boom is initially at rest,

$$\alpha = \frac{2(\theta_f - \theta)}{t_{sep}^2}$$

Using Equation (4), the above equation can be transformed to

$$\alpha = \frac{2(\theta_{cf} - \theta_c)}{t_{sep}^2} \tag{5}$$

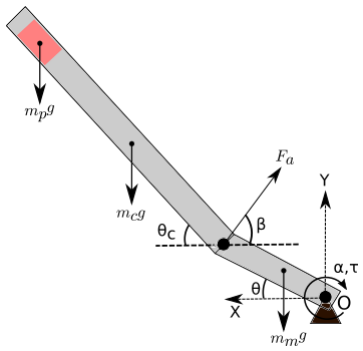

Fig. 3. Free body diagram of the boom at Launchpad condition

2.4. Rigid body dynamics

The equation of motion for the boom is developed based on torque balance about pivot point of the boom, origin 'O' of XY co-ordinate system (Fig. 3), for launch pad abort condition. The additional inertial forces, due to acceleration of the vehicle, also plays a role in the dynamics of boom and shall be incorporated in parameter 'g'. As there is no loss in generality, the present study does not account for such inertial force. Considering rotational analogue of Newton's second law of motion [6], the torque (τ) acting on the boom is expressed about origin 'O'.

$$\begin{aligned} \sum \tau &= I\alpha \\ F_a \sin(\theta+\beta)\, l_m - F_g x_{cg} &= I\alpha \\ F_a \sin(\theta+\beta)\, l_m - mg x_{cg} &= I\alpha \end{aligned} \tag{6}$$

Re-arranging Equation (6), the force required from actuator is expressed as

$$F_a = \frac{I\alpha + mg x_{cg}}{l_m \sin(\theta+\beta)} \tag{7}$$

3. Problem Formulation

The objective of the present study is to minimize the force required to rotate the boom structure for effective separation of CM and SM. The optimization problem is formalized as following

$$Minimize:\ F_a = \frac{I\alpha + mg x_{cg}}{l_m \sin(\theta+\beta)} = f(l_m, \theta, \beta) \tag{8}$$

where, I, m and x_{cg} are as per Eq. (1), Eq. (2) and Eq. (3) respectively.

$$\begin{aligned} Subject\ to: g_1 = X_{max} - X_{sp} - l_m \cos\theta &\geq 0 \\ g_2 = X_{sp} \tan\beta - Y_{gap} &\geq 0 \\ g_3 = Y_{max} - l_c \sin\theta_c - l_a \sin\beta &\geq 0 \\ \theta_{cf} &= 106^o \\ t_{sep} &\leq 0.150 \end{aligned} \tag{9}$$

The constraints, g_1, $g_2, and\ g_3$, are geometric in nature and derived from the space limitation of the launch vehicle. In contrast, θ_{cf} and t_{sep} are functional constraints from mission point of view and these need to be satisfied for ensuring clean separation of crew module from service module. The optimization problem, defined by Equations (8) and (9), belongs to parameter or static optimisation case. The variables involved in the optimization problem can be categorised in "decision variables", "preassigned parameters" and "derived parameters".

Decision Variables: l_m, θ, β
Preassigned Parameters: m_m, m_c, m_p, l_c, X_{sp}, Y_{gap}, θ_c, α
Derived Parameters: α, l_a, X, Y, Y_{sp}

Using (5) and mission constraints from (9),

$$\alpha = \frac{2 \times (106-76) \times \pi}{0.15^2 \times 180} = 23\ rad/s^2 \tag{10}$$

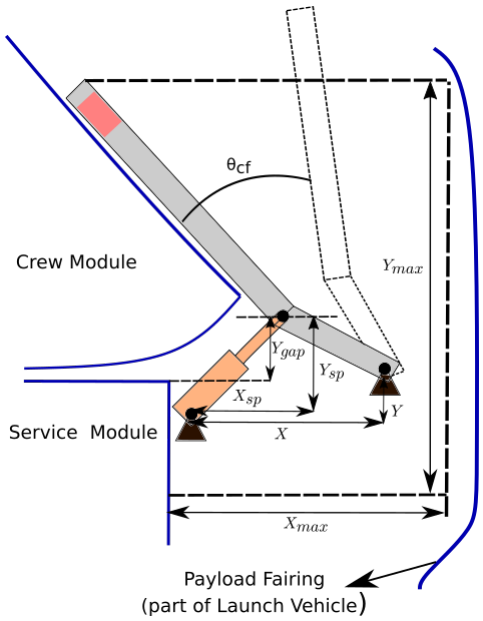

Fig. 4. Geometric Constraints due to Launch Vehicle

Table 1. Input parameters for optimization study

m	50 kg
m_m	$0.1m$ = 5 kg
m_c	$0.2m$ = 10 kg
m_p	$0.7m$ = 35 kg
l_c	650 mm
X_{sp}	175 mm
Y_{gap}	450 mm
θ_c	76°
X_{max}	330 mm
Y_{max}	1090 mm

Considering uncertainity in the input variables and to be more conservative, the above value is rounded off to 30 rad/s^2.
The remaining parameters in this group depends on the decision variables and are computed in Section 5.

$$\begin{aligned} l_a &= \frac{X_{sp}}{\cos\beta} \\ X &= X_{sp} + l_m\cos\theta \\ Y &= l_a\sin\beta - l_m\sin\theta \\ Y_{sp} &= X_{sp}\tan\beta \end{aligned} \tag{11}$$

4. Optimization Study

The optimization is carried out for both unconstrained and constrained case. The computations are carried out in *SciPy Ver. 1.1.0* scientific computing package [7] of *Python Ver. 3.7.1* platform. *Python* is an open-source general-purpose programming language with support for scientific computation and data visualization tools. The minimization of the objective function, for the present study, is carried out using *scipy.optimize* which provides following subroutines for multivariable nonlinear optimization of scalar objective functions.

1. *scipy.optimize.minimize*: This functions provides various standard algorithms like 'Nelder-Mead', 'Powell', 'CG' methods, 'COBYLA' etc. for both unconstrained and unconstrained cases.

2. Global Optimization: *scipy.optimize* contains algorithms like Basin-Hopping, Differential Evolution, SHG, Dual Annealing and brute force for finding global minimum of multivariate function.

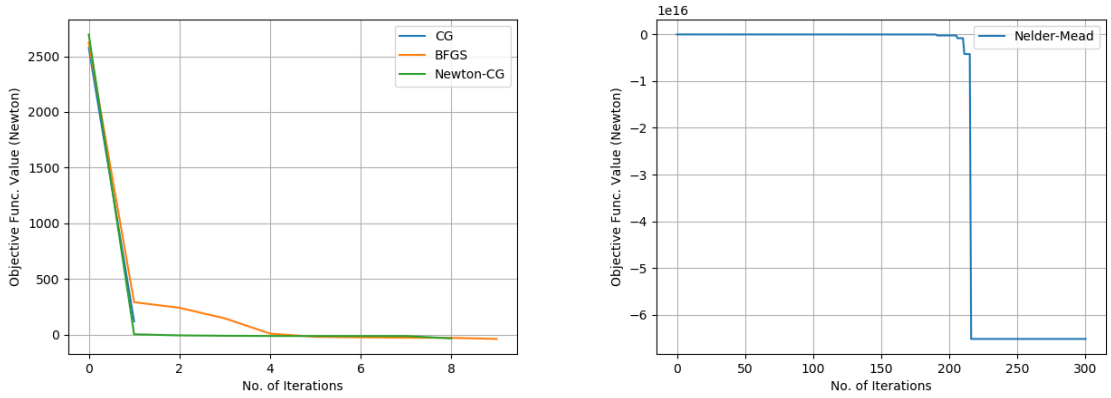

(a)Loss of precision (b)Converged with $\nabla f \neq 0$

Fig. 5. Results of unconstrained optimization

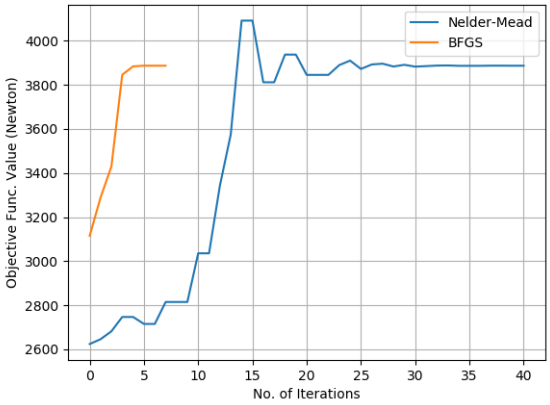

Fig. 6. Performance of optimization algorithm with 2 decision variables

Case 1: Unconstrained Optimization

Necessary and Sufficient conditions for local minimum [8]:

$$\begin{aligned} \nabla f(X^*) &= 0 \\ \nabla^2 f(X^*) &\succ 0 \end{aligned} \tag{12}$$

The unconstrained case is solved numerically using both direct search and descent methods implemented in *scipy.optimize.minimize* module. It is found that the above problem is ill-posed and no solution found with three independent decision variables, l_m, θ, *and* β. Most of the algorithms did not converge to solution citing loss of precision and sample results are shown in Fig. 5. As evident from Fig. 5(a), the value of objective function falls rapidly and goes to negative side before stopping due to loss of precision. In Fig. 5(b), the function value dwells at zero before falling to -6.5×10^{16}.

Based on the above results, the minimization approach is modified by reducing the number of decision variable to 2 Nos., l_m, *and* θ. β is excluded as it appears only in one place in the expression of objective function (Eq. (7)) and does not effect physical parametrs like CG and MI. Moreover, β can be separately controlled independent of boom structure. With β as input parameter, the algorithms converges and results are shown in Fig. 6. The results clearly shows that 'Nelder-Mead' algorithm which is a direct search method takes more number of iteration compared to gradient based methods like 'BGFS' to arrive at optimum value. Both the algortihms are initiated with same intial condition, $l_m = 0.7$ *m* and $\theta = 20°$. The Table 2 shows the optimum values of decision variables, l_m and θ, for minimum actuator force, F_a, corresponding to various β. It is concluded that there is no local minimum of F_a with respect to β. The negative values of θ are discarded as they represent un-realistic scenarios for our case. Hence, the minimum possible value for F_a lies between $\beta = 60^o$ and $\beta = 70^o$. The θ in this range of β is nearly equal to zero i.e. the bent arm

Table 2. Minimum F_a for range of β

β (deg.)	l_m (mm)	θ (deg.)	F_a (kN)
10	509.07	102.90	2.64
20	509.07	82.82	2.79
30	509.07	62.74	2.86
40	509.07	42.67	2.84
50	509.07	22.59	2.73
60	509.07	2.50	2.54
70	509.07	-17.59	2.27
80	509.07	-37.74	1.93
90	509.07	-57.94	1.53

Table 3. Results of Global Optimization

Paramters	Bounds	Optimum Value
l_m	100 to 900 mm	509.07 mm
θ	0 to 90°	0°
β	0 to 90°	90°
F_a	Not Applicable	2.20 kN

is almost horizontal. Clearly, the outcome of the unconstrained optimization does not meet the horizontal constraint of X_{max} (constraint g_1).
The above behaviour is further confirmed by 'Differential Evolution' alogrithm for global optimization. The bounds for decision variables were chosen judiciously to allow for practical solutions. The algorithm converges with non-zero jacobian, suggesting non-existence of any relative minimum in the design space. The outcome (Table 3) is inline with the unconstrained optimization result, if the negative values of θ are neglected for the later case.

Case 2: Constrained Optimization

As mentioned in Section 3, constraints are of inequality type and Kuhn-Tucker conditions need to be satisfied [8] for obtaining minimum of F_a (Eq. (8)). It is observed from the unconstrained optimization study (Case 1) that the problem is ill-posed with no relative minimum. The 'SLSQP' method is employed with three decision variables viz. l_m, θ, β, considering the flexibility of imposing bounds via *scipy.optimize.minimize* function. The inequality constraints are applied as per Eq. (9).
Bounds: $l_m = [0\ mm, 600\ mm]$, $\theta = [0°, 150°]$, $\beta = [40°, 90°]$
Initialization vector: $l_m = 100\ mm$, $\theta = 30°$, $\beta = 70°$
The 'SLSQP' algorithm took 16 iterations, refer Fig. 7, to converge at the solution given in Table 4.
The above solution is verified explicilty for compliance of constraints and the results are shown in Table 5.

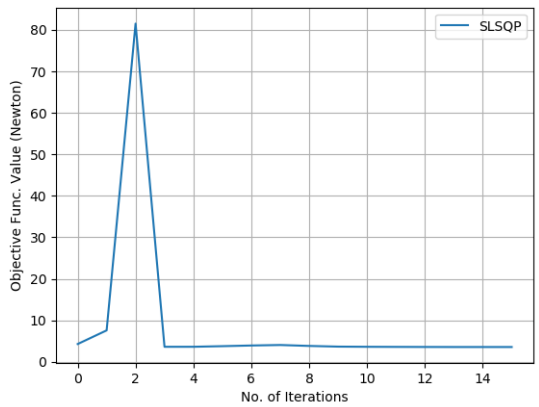

Fig. 7. Convergence of SLSQP algorithm

Table 4. Optimum solution with constraints

Parameter	Optimum Value
l_m	156.5 mm
θ	7.95°
β	69.14°
F_a	3.56 kN

Table 5. Constraints corresponding to optimal solution

Constraints	Value at X*
g_1	1.56×10^{-8} mm
g_2	9.31 mm
g_3	2.56×10^{-10} mm

5. Results and Discussions

As shown by the unconstrained and global optimization study in previous section, the optimization problem of boom-actuator system, with three decision variables, is an ill-posed one. The outcome of the global optimization,θ = 0° and $\beta = 90°$, is an intiuitive one. Observing the objective function (Eq. (8)), it is indicative (not obvious and necessary) that actuator force minimizes as $\theta + \beta = 90°$. However, solving the problem under constraints resulted in viable solution which can be implemented for human spaceflight program.

1. Based on the results obtained from constrained optimization study, the derived parameters are computed using Eq. (4) and (11). Table 4 and Table 6 provides all parameters (Fig. 2(b)) to define the actuator-boom configuration as modeled for the present study.

2. A single bracket structure is proposed to mount the actuator and boom. The bracket is rigidly fixed to service module structure. $X = 329.9$ mm and $Y = 437.6$ mm represents the overall envelope of the bracket to be designed. It is observed that the horizontal span of the bracket is equal to maximum space constraint in the horizontal direction. So, it is prudent to keep some margin with actual vehicle envelope prior to optimization study.

3. Cutout in SM need to be configured to route the fluid/electrical lines through bracket to the boom and finally to CM. Flexible hoses are the first choice for fluid lines considering the movement required during separation. However, caution shall be taken to bend the hoses properly in a smooth manner around the bracket-boom structure. An alternative is to use combination of flexible hoses and rigid tubes. Flexible hoses shall be used from SM to boom bottom, facilitating the movement during separation. Rigid tubes over the boom is preferable as there is no relative movement required in this part during separation.

4. The minimum force to be delivered by actuator is found to be 3.56 kN (Table 4). The geometric length, l_a may not be considered as intial length (non-actuated condtion) of the actuator. The actuator can be smaller than the optimum value of 491.5 mm. This means that the actuator to be mounted on passive structure to satisfy the geometric constraint of 491.5 mm.

5. The minimum force obtained from constrained optimization is applicable only for the initial condition when the umbilical system is mated with CM. The variation of force requirement due to movement of umbilical system

Table 6. Derived Parameters corresponding to Optimum solution

Parameter	Optimum Value
l_a	491.5 mm
X	329.9 mm
Y	437.6 mm
Y_{sp}	459.3 mm
θ_f	37.95°

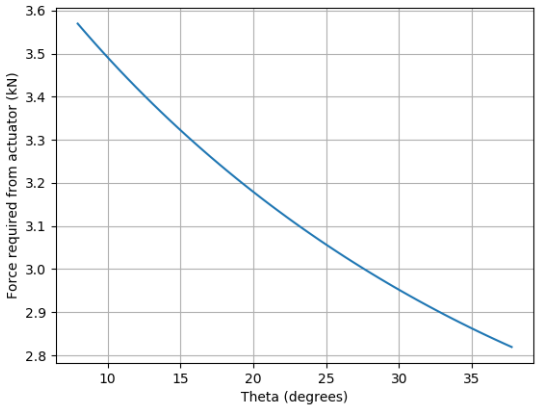

Fig. 8. Force required from Actuator during separation

is necessary to design the actuator. Expression of X and Y (Eq. (9)) can be manipulated to lead to following geometric relation.

$$\tan\beta = \frac{Y + l_m \sin\theta}{X - l_m \cos\theta} \tag{13}$$

Using Eq. (7) and (13), the force required by actautor is plotted for $\theta = 7.95^\circ$ to 37.95° (Fig. 8).

6. Conclusion

A simplified dynamic model, of the proposed actuator-boom configuration, is formulated based on relevant assumptions. The actuator-boom configuration is optimized considering constraints from mission and launch vehicle. As there is no general rule to select the best algorithm, it is recommended to explore the behaviour of objective function using various available algorithm. In this case, the objective function is explored using unconstrained, global and constrained optimization techinques. It is also shown that even in case of ill-posed enigneering problem, feasible solutions are possible within the specified geometric and functional constraints. The implementation of the obtained results to actual hardware is also discussed in brief. It is noted that the present study does not take into account inertial forces due to launch vehicle motion. This study can be further modified to include structure dynamic aspects of boom.

References

[1] Department of Space, Government of India, Annual Report 2018-2019, https://www.isro.gov.in/sites/default/files/annualreport2018-19.pdf , 2019.
[2] NASA, CSM Overview, https://www.hq.nasa.gov/alsj/CSMNewsRef-Boothman.html.
[3] Damon Delap, Joel Glidden and Christopher Lamoreaux, Development of the Orion Crew-Service Module Module Umbilical Retention and Release Mechanism, John Wiley, 15th European Space Mechanisms and Tribology Symposium, Vol. 718 (2013).
[4] Jiaqi Xu, and Hwan-Sik Yoon, A review on mechanical and hydraulic system modeling of excavator manipulator system, Journal of Construction Engineering 2016 (2016).
[5] Leszek Cedro, Linearization and identification a Mathematical model of an excavator, Proceedings of the 2014 15th International Carpathian Control Conference (ICCC), IEEE (2014) 73-79.
[6] D. Halliday, R. Resnick and J. Walker, Fundamentals of Physics, John Wiley & Sons, 2010
[7] Pauli Virtanen, Ralf Gommers, et. al., and SciPy 1.0 Contributors. Scipy 1.0–fundamental algorithms for scientific computing in python. arXiv e-prints, page arXiv:1907.10121, Jul 2019.
[8] S.S. Rao, Engineering Optimization: Theory and Practice, New Age International, 2006